

# Plasmonic Helicity-Driven Detector of Terahertz Radiation

I.V. Gorbenko,<sup>1</sup> V. Yu. Kachorovskii,<sup>1,2</sup> and M. S. Shur<sup>3</sup>

<sup>1</sup>*A. F. Ioffe Physico-Technical Institute, 194021 St. Petersburg, Russia*

<sup>2</sup>*L. D. Landau Institute for Theoretical Physics, Kosygina street 2, 119334 Moscow, Russia*

<sup>3</sup>*Rensselaer Polytechnic Institute, 110, 8<sup>th</sup> Street, Troy, NY, 12180, USA*

(Dated: July 17, 2018)

We develop a theory of the helicity driven nonlinear dc response of gated two-dimensional electron gas to the terahertz radiation. We demonstrate that the helicity-sensitive part of the response dramatically increases in the vicinity of the plasmonic resonances and oscillates with the phase shift between excitation signals on the source and drain. The resonance line shape is an asymmetric function of the frequency deviation from the resonance. In contrast, the helicity-insensitive part of the response is symmetrical. These properties yield significant advantage for using plasmonic detectors as terahertz and far infrared spectrometers and interferometers.

Plasma wave terahertz (THz) emitters [1–7] and detectors [8–24] based on field effect transistors (FETs) are promising candidates for filling the famous THz gap. Although the emission of radiation requires some special conditions, particularly, specific boundary conditions (BC) [1] or the electron velocity exceeding the plasma velocity [25] the detection only relies on the device non-linearity [8]. Impinging THz or sub-THz radiation excites plasma waves in the FET channel. Rectification of these waves leads to a voltage drop across the structure. The effect was first described in Ref. [8] within the hydrodynamic approach, which is applicable for the systems operating in the electron-electron collision dominated regime. The properly designed two-dimensional (2D) plasmonic structures yield superior detection of the THz radiation [26–34]. THz detectors based on GaAs [10–21], Si [22, 23] and GaN [13, 24] FETs have already achieved performance comparable to or even exceeding that of commercial detectors, demonstrating tunability [8–24], a relatively low value of the noise equivalent power [23, 24], a potential to detect signals with very high modulation frequencies (up to hundreds of GHz) [35], and operation in heterodyne and homodyne regimes [36–41] with a very high responsivity. Such detectors can operate both at zero bias current, with a minimum shot noise, and in the regime of a relatively large drain-to-source current. In the latter case, the detection efficiency can be significantly improved due to the current-driven increase of nonlinear properties of the channel [11, 19]. Also, as any nonlinear elements, plasmonic detectors can operate as frequency mixers or frequency multipliers [8]. Using multi gate detectors based on the ratchet effect (see Refs. [42–46] and references therein) further improves the detector performance.

Recently, we studied the THz homodyne detection in the strongly non-perturbative, with respect to radiation power, regime [41] (see also previous publications on homodyne detection [36–40] and on the non-perturbative response [47–49]). We found the upper bound for the rectified response, which exceeds the conventional perturbative response by orders of magnitude. Most importantly, we also demonstrated that, apart from the ex-

tremely high sensitivity, this regime of operation allows for the direct measurements of the phase difference between a weak incoming signal and the local oscillator signal. In other words, the homodyne response encodes the information about the phase difference between the two signals (see also [37]). This property enables using plasmonic detectors as THz and far infrared spectrometers and interferometers.

Here, we show that helicity driven response could also enable the application of the *resonant* plasmonic detectors as tunable THz spectrometers and interferometers. Helicity-driven *non-resonant* effects were observed earlier in Ref. [50] and explained in [51]. They were predicted to be absent for zero loading impedances [51]. Below, we demonstrate that in the resonant regime, the intrinsic FET channel shows the helicity-driven response.

We start from recalling that plasma waves in a gated two-dimensional structure biased above threshold, have a linear dispersion law  $\omega(k) = sk$ , [52] where

$$s = \sqrt{\frac{eU_g}{m}} \quad (1)$$

is the wave velocity, which along with the electron concentration in the channel,

$$N = \frac{CU_g}{e}, \quad (2)$$

is controlled by the gate-to-channel swing  $U_g$  counted from the FET threshold voltage [in Eq. (2) we assume that  $U_g$  is positive and much larger than the thermal voltage]. Here  $C = \epsilon/4\pi d$  is the gate to channel capacitance per unit area,  $e$  is the electron charge,  $m$  is the electron effective mass,  $d$  is the gate-to-channel distance and  $\epsilon$  is the dielectric constant. For low electron scattering rates, a structure of a given length,  $L$ , acts for plasma waves as a resonant "cavity", with resonant frequencies

$$\omega_N = \omega_0(N + a), \quad (3)$$

where  $\omega_0 = \pi s/L$ ,  $N = 0, 1, 2, \dots$ , and  $a$  is numerical coefficient which depends on BC:  $a = 1/2$  for voltage fixed at the source and current fixed at the drain [1] and

$a = 0$  for voltage fixed both at the source and at the drain (for  $a = 0$ , the mode with  $N = 0$  corresponds to the Drude peak discussed at the end of the paper). In a short channel FET, the oscillation frequency,  $\omega_0/2\pi$ , can be tuned by  $U_g$  to be in THz range.

A quality factor of the cavity is given by  $\omega_0\tau$ , where  $\tau$  is the momentum relaxation time. Depending on the value of the quality factor and excitation frequency, transistor can operate in the resonant,  $\omega \approx \omega_0 \gg 1/\tau$ , and non-resonant regimes. In the latter case, the plasma oscillations are overdamped. The dramatic reduction of the device sizes in the last decades has led to the development of the new generations of FETs, which may have high quality factors. Such FETs should demonstrate novel physics, specific for the ballistic regime. In particular, the response of such FET to an external radiation shows sharp resonances. Typically, these resonances are well described by the *symmetric* Lorentz peaks insensitive to the radiation polarization [8]. One of the purposes of this paper is to demonstrate that excitation by a circularly-polarized wave can result in the helicity-sensitive resonant response with an *asymmetric* line shape. We assume that the electron-electron collisions are very fast turning the system into the hydrodynamics regime. The hydrodynamic equations describing a two-dimensional electronic fluid in FET channel read

$$\frac{\partial v}{\partial t} + v \frac{\partial v}{\partial x} + \gamma v = -\frac{e}{m} \frac{\partial U}{\partial x}, \quad (4)$$

$$\frac{\partial U}{\partial t} + \frac{\partial(Uv)}{\partial x} = 0, \quad (5)$$

where  $v$  is the velocity of the electronic fluid, and  $U$  is the local value of the gate-to-channel voltage, which, in the gradual channel approximation, is related to the local value of the electron concentration as  $N(x) = CU(x)/e$  [1]. The rate of the velocity relaxation is determined by the inverse momentum relaxation time  $\gamma = 1/\tau$ . Actually, there is also some momentum-dependent contribution to the relaxation rate,  $\eta k^2 \sim \eta/L^2$ , caused by the viscosity  $\eta$  of the electron fluid [1]. Here, we neglect this contribution assuming that  $L^2 \gg \eta\tau$ . We also assume that channel is sufficiently wide and do not discuss the effects related to the friction of the viscous electron fluid at the boundaries of the sample.

Eqs. (4) and (5) require two BC, which depend on the properties of contacts. In the first publications on the plasma-wave non-linear detection Ref. [1], [8] it was assumed that the ac voltage  $U_a$  is applied at the source side of the channel and the current flowing through the FET is fixed at the drain side of the channel. Physically, this implies the infinite inductive loading impedance on the drain side of the channel. It was shown [8] that rectification of the ac oscillations induces a constant source-to-drain voltage:  $V \propto U_a^2$  at low intensities of excitation [8] and  $V \propto U_a$  at higher intensities [41, 47–49].

Here, we consider the BC corresponding to a different physical situation [50, 51]. We assume that the circu-

larly polarized radiation excites a sample via two antennas coupled to the source and drain. Hence, ac signals at the source and drain have equal frequencies but can be shifted by phase with the shift magnitude  $\theta$  determined by antenna design and have different amplitudes. Taking into account that the radiation induces a dc voltage drop  $V$  across the sample, we write the BC as follows

$$\begin{aligned} U(0) &= U_g + U_a \cos(\omega t + \theta), \\ U(L) &= U_g + V + U_b \cos \omega t. \end{aligned} \quad (6)$$

In the case, when the device is excited by a circularly polarized wave,  $\theta$  changes sign with changing the helicity of the polarization [50, 51]. We focus on the helicity-driven effects, i.e. on the contribution to the current, which changes sign with replacing  $\theta$  with  $-\theta$  or, equivalently,  $\omega$  with  $-\omega$  (for definiteness we put below  $\omega > 0$ ). We will derive general equation for the dc response valid both in resonant and non-resonant cases, and find that in all cases helicity-dependent part of the response is given by

$$J_{\text{hel}} \propto \sin \theta U_a U_b. \quad (7)$$

We will show that the coefficient in this equation dramatically increases in vicinity of plasmonic resonances [53] as compared to non-resonant case discussed in Refs. [50, 51].

We first introduce the dimensionless variable  $n = (U - U_g)/U_g$  and search for the solution of Eqs. (4),(5) in the following form

$$n = n_0(x) + \frac{1}{2}n_1(x)e^{-i\omega t} + \frac{1}{2}n_{-1}(x)e^{i\omega t} + \dots, \quad (8)$$

$$v = v_0(x) + \frac{1}{2}v_1(x)e^{-i\omega t} + \frac{1}{2}v_{-1}(x)e^{i\omega t} + \dots, \quad (9)$$

where  $n_0(x) = \langle n(x, t) \rangle_t$  and  $v_0 = \langle v(x, t) \rangle_t$  are the time-averaged potential and velocity, respectively, and  $n_1$  and  $v_1$  are small ( $\propto U_{a,b}$ ) radiation-induced plasmonic oscillations. In the absence of radiation,  $n_0 = 0, v_0 = 0$ , while in the presence of radiation they are quadratic with respect to the wave amplitude ( $\propto U_{a,b}^2$ ).

Substituting Eqs. (8) and (9) into Eqs. (4), (5) and averaging over time we get

$$\frac{\partial}{\partial x} \left( \frac{v_0^2}{2} + \frac{v_1 v_{-1}}{4} + s^2 n_0 \right) + \gamma v_0 = 0, \quad (10)$$

$$\frac{\partial}{\partial x} \left[ (1 + n_0)v_0 + \frac{n_1 v_{-1} + n_{-1} v_1}{4} \right] = 0. \quad (11)$$

Since the voltage is fixed at the source, the BC at the source is  $n_0(0) = 0$ . By solving these equations, one can find the radiation-induced voltage drop across the sample,  $V = U_g[n_0(L) - n_0(0)] = U_g n_0(L)$ . In Eqs. (10), (11), one can neglect small terms  $\partial v_0^2/\partial x$  and  $\partial(v_0 n_0)/\partial x$  [54]. For zero dc current, we find from Eq. 11  $v_0 = -(n_1 v_{-1} + n_{-1} v_1)/4$ . Substituting this equation into Eq. 10 we find

$$\begin{aligned} \frac{V}{U_g} &= \frac{1}{4s^2} \left[ \gamma \int_0^L dx (n_1 v_{-1} + n_{-1} v_1) \right. \\ &\quad \left. + v_1(0)v_{-1}(0) - v_1(L)v_{-1}(L) \right]. \end{aligned} \quad (12)$$

Next, one should find  $n_1$  and  $v_1$  and substitute into Eq. (12). One can see that the variations of  $n_0$  and  $v_0$  are small and can be neglected in quadratic in  $U_{a,b}$  approximation provided that there is no dc current in the channel. Therefore, in equations for  $n_1$  and  $v_1$  we can assume  $n_0 = \text{const}$ ,  $v_0 = \text{const}$ . Since the dc current in the channel is zero, we put  $v_0 = 0$ . One can also assume in these equations  $n_0 = 0$ , since spatially independent concentration is fully controlled by  $U_g$ . Then, we get

$$(\gamma - i\omega)v_1 + s^2 \frac{\partial n_1}{\partial x} = 0 \quad (13)$$

$$-i\omega n_1 + \frac{\partial v_1}{\partial x} = 0. \quad (14)$$

In the infinite system, the solutions of Eqs. (13), (14) are harmonic plasma waves  $n_1, v_1 \sim e^{\pm ikx}$ , with

$$k = \frac{\sqrt{\omega(\omega + i\gamma)}}{s} = \frac{\Omega + i\Gamma}{s}. \quad (15)$$

Here,  $\Omega = s(k + k^*)/2$ ,  $\Gamma = s(k - k^*)/2i$  are the plasma wave frequency and damping, respectively.

The solution of Eqs. (13) and (14) in the finite system of length  $L$  with the BC (6) reads

$$n_1 = (Ae^{ikx} + Be^{-ikx}), \quad (16)$$

$$v_1 = \frac{\omega}{k} [Ae^{ikx} - Be^{-ikx}], \quad (17)$$

where

$$A = \frac{U_b e^{-i\theta_b} - U_a e^{-i\theta_a} e^{-ikL}}{2iU_g \sin(kL)}, \quad (18)$$

$$B = \frac{U_a e^{-i\theta_a} e^{ikL} - U_b e^{-i\theta_b}}{2iU_g \sin(kL)}. \quad (19)$$

Substituting Eqs. (17) and (16) into Eq. (12), we find

$$V = \frac{\omega}{\sqrt{\omega^2 + \gamma^2}} \frac{\alpha(U_a^2 - U_b^2) + \beta U_a U_b \sin \theta}{4U_g |\sin(kL)|^2}, \quad (20)$$

where

$$\alpha = \left(1 + \frac{\gamma\Omega}{\Gamma\omega}\right) \sinh^2\left(\frac{\Gamma L}{s}\right) - \left(1 - \frac{\Gamma\gamma}{\Omega\omega}\right) \sin^2\left(\frac{\Omega L}{s}\right), \quad (21)$$

$$\beta = 8 \sinh\left(\frac{\Gamma L}{s}\right) \sin\left(\frac{\Omega L}{s}\right). \quad (22)$$

Equation (20) is valid for an arbitrary relation between  $\omega, \omega_0$  and  $\gamma$ . Different regimes of operation are illustrated in Fig. 1. Below we discuss these regimes in detail.

### 1. Non-resonant case, $\omega \ll \gamma$ (grey area in Fig. 1).

In this case, from Eq. (15), we find:  $\Omega \approx \Gamma \approx \sqrt{\omega\gamma}/2$ , which means that the plasma waves are overdamped. It is convenient to introduce the characteristic length [8, 19]

$$L_* = \frac{s\sqrt{2}}{\sqrt{\omega\gamma}} = \frac{s}{\Gamma}. \quad (23)$$

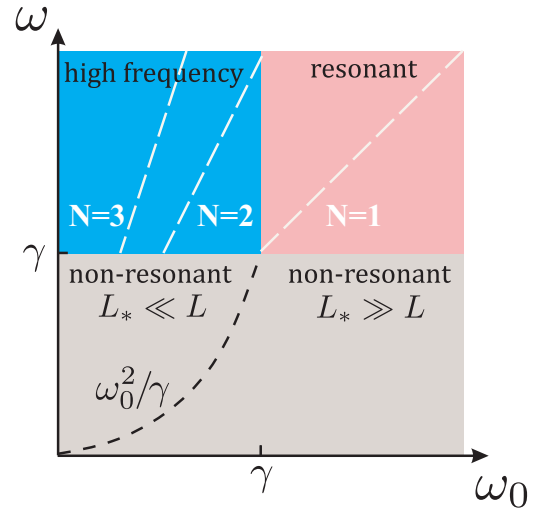


FIG. 1. Different regimes of detector operation.

The plasma excitations exponentially decay at the scale  $L_*$  from the edges of the sample to the bulk. One can, therefore, consider two limiting cases of the long and short samples:

a. *Long sample*,  $L \gg L_*$  ( $\omega \gg \omega_0^2/\gamma$ ). In this case, Eq. (20) simplifies

$$V = \frac{U_a^2 - U_b^2 + 16U_a U_b e^{-L/L_*} \sin(L/L_*) (\omega/\gamma) \sin \theta}{4U_g}. \quad (24)$$

The helicity-sensitive term is exponentially small. This is because helicity-dependent contribution arises due to the coupling between the source and drain, which is suppressed in the long sample.

b. *Short sample*,  $L \ll L_*$  ( $\omega \ll \omega_0^2/\gamma$ ). In this case, the response reads

$$V = \frac{U_a^2 - U_b^2 + 4U_a U_b (\omega/\gamma) \sin \theta}{4U_g}. \quad (25)$$

Let us compare Eqs. (24) and (25) with the analytical results obtained in Ref. [51], which was focused on the study of the non-resonant case. Their analysis demonstrated that a non-zero contribution to the helicity-sensitive part of the response appears only for non-zero loading impedance  $Z$ . Since in our case  $Z \equiv 0$ , it seems that there is contradiction between the results. This contradiction is resolved by noticing that in Eqs. (24) and (25) the helicity-driven contribution contains a factor  $\omega/\gamma$  which is small in the non-resonant approximation. The non-resonant equations used in Ref. [51] neglect such terms. In other words, the terms, which are proportional to  $\sin \theta$ , appear in Eqs. (24) and (25) as corrections to pure non-resonant approximation. It worth stressing that in a short sample the helicity-driven contribution is not exponentially small and, therefore, can be observed experimentally.

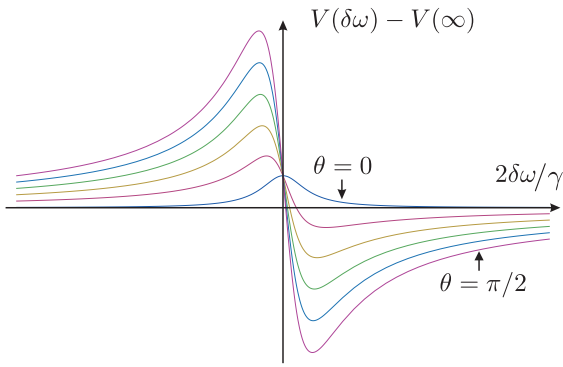


FIG. 2. Resonant dependence of response on the radiation frequency [Eq. (27)] at different  $\theta$  varying from 0 to  $\pi/2$  for  $U_a U_b / (U_a^2 - U_b^2) = 5$  and  $N = 1$ . With increasing  $\theta$  asymmetry of the resonance is enhanced due to increasing of the helicity-sensitive contribution.

### 2. High frequency case, $\omega_0 \ll \gamma \ll \omega$ (blue area in Fig. 1).

In this case,  $\Omega \approx \omega$ ,  $\Gamma \approx \gamma/2$ . The response is given by

$$V = \frac{3(U_a^2 - U_b^2)}{4U_g} + \frac{4U_a U_b e^{-\gamma L/2s} \sin(\pi\omega/\omega_0) \sin\theta}{U_g}. \quad (26)$$

Similar to Eq. (24), the helicity-dependent contribution in Eq. (26) is exponentially small, since  $\gamma L/s \sim \gamma/\omega_0 \gg 1$ . However, the frequency dependencies of these equations are essentially different: linear in Eq. (24) and periodic in Eq. (26).

### 3. Resonant case, $\omega \gg \gamma$ , $\omega_0 \gg \gamma$ (pink area in Fig. 1)

Similar to the previous case,  $\Omega \approx \omega$ ,  $\Gamma \approx \gamma/2$ . The response shows series of the sharp peaks at  $\omega = \omega_N$ . In the vicinity of  $N$ -th resonance ( $N \neq 0$ ), we find

$$V(\delta\omega) = \frac{(U_a^2 - U_b^2)(3\gamma^2/4 - \delta\omega^2) + 4U_a U_b (-1)^N \delta\omega \gamma \sin\theta}{4U_g(\delta\omega^2 + \gamma^2/4)} \quad (27)$$

where  $\delta\omega = \omega - \omega_N$  and resonant frequencies are given by  $\omega_N = \pi N s / L$  for BC Eq. (6) [ $a = 0$  in Eq. (3)].

The most intriguing property of Eq. (27) is an asymmetrical resonance dependence on the frequency of the incoming radiation. More specifically, the response is given by the sum of two parts sharply peaked at  $\delta\omega = 0$ : conventional, polarization-independent part, which obeys

the symmetry  $\delta\omega \rightarrow -\delta\omega$ , and helicity-driven part which changes sign under this operation. The latter increases with increasing the phase shift  $\theta$ . This property is illustrated in Fig. 2, where response is shown for fixed  $\gamma$  and  $U_{a,b}$  but for different phase shifts  $0 < \theta < \pi/2$ . As seen, asymmetrical part of the response increases with increasing  $\theta$ . Hence, conventional and helicity-driven contributions can be easily separated by measuring the frequency dependence of the response.

### 4. Drude peak

Finally, we consider in more detail what happens when  $\omega_0 \gg \gamma$  and  $\omega$  increases from small values  $\omega \ll \gamma$  to relatively large value  $\omega_0 \gg \omega \gg \gamma$  (moving from grey to pink area in Fig. 1). In other words, we consider response for  $\omega \approx \omega_N$  with  $N = 0$ . Simple analysis of Eq. (20) yields the peak of the width  $\gamma$  (Drude peak)

$$V(\omega) = \frac{(U_a^2 - U_b^2)(\gamma^2 - \omega^2) + 4U_a U_b \omega \gamma \sin\theta}{4U_g(\omega^2 + \gamma^2)}. \quad (28)$$

For  $\omega \ll \gamma$  this equation simplifies to Eq. (25).

Comparing Eqs. (27) and (28), we find that the Drude peak is very similar to the plasmonic resonances. However, symmetrical and asymmetrical parts of the Drude peak are, respectively, 3 and 4 times smaller.

To conclude, the theory of nonlinear resonant plasmonic response of the gated 2D electron gas subjected to THz radiation with a given helicity shows that the helicity-driven contribution dramatically increases in the vicinity of the plasmonic resonances. This contribution is a harmonic function of the phase shift and shows an asymmetric dependence on the excitation frequency in the vicinity of the resonances. Hence it can be easily separated from conventional symmetric contribution, which is not sensitive to radiation polarization. Helicity-sensitive contribution can also be observed in the non-resonant regime. Although it is small in this case as compared to polarization insensitive part of the response, it has easily identifiable frequency and phase dependence and, therefore, can be experimentally separated.

The work of M. S. S. was supported by the U.S. Army Research Laboratory through the Collaborative Research Alliance for Multi-Scale Modeling of Electronic Materials and by the Office of the Naval Research (Project Monitoe Dr. Paul Maki). The work of V. Yu. K. was supported by Russian Science Foundation (grant No. 16-42-01035). The work of I.V.G. was supported by the Foundation for the advancement of theoretical physics BASIS.

- 
- [1] M. Dyakonov and M. S. Shur, Phys. Rev. Lett. **71**, 2465 (1993).  
 [2] A.P. Dmitriev, V.Yu. Kachorovskii, and M.S. Shur, Appl. Phys. Lett. **79**, 922 (2001).  
 [3] A.P. Dmitriev, A.S. Furman, and V.Yu. Kachorovskii,

- Phys. Rev. B **54**, 14020 (1996).  
 [4] A.P. Dmitriev, A.S. Furman, V. Yu. Kachorovskii, G.G. Samsonidze, and Ge.G. Samsonidze, Phys. Rev. B **55**, 10319 (1997).  
 [5] W. Knap, J. Lusakowski, T. Parenty, S. Bollaert, A.

- Cappy, V. Popov, M.S. Shur, Appl. Phys. Lett. **84**, 2331 (2004).
- [6] Y. Deng, R. Kersting, J. Xu, R. Ascazubi, Xi. Zhang, M.S. Shur, R. Gaska, G.S. Simin, M. Asif Khan, and V. Ryzhii, Appl. Phys. Lett., **84**, 70 (2004).
- [7] N. Dyakonova, A. El Fatimy, J. Lusakowski, W. Knap, M. I. Dyakonov, M.-A. Poisson, E. Morvan, S. Bollaert, A. Shchepetov, Y. Roelens, Ch. Gaquiere, D. Theron, and A. Cappy, Appl. Phys. Lett. **88**, 141906 (2006).
- [8] M. Dyakonov and M.S. Shur, IEEE Transaction on Electron Devices **43**, 380 (1996).
- [9] R. Weikle, J. Lu, M.S. Shur, M.I. Dyakonov, Electronics Letters **32**, 2148 (1996).
- [10] J. Lu, M.S. Shur, J.L. Hesler, L. Sun, and R. Weikle, IEEE Electron Device Letters **19**, 373 (1998).
- [11] J.Q. Lü and M.S. Shur, Appl. Phys. Lett. **78**, 2587 (2001).
- [12] W. Knap, S. Romyantsev, J. Lu, M. Shur, C. Saylor, and L. Brunel, Appl. Phys. Lett., **80**, 3433 (2002).
- [13] W. Knap, V. Kachorovskii, Y. Deng, S. Romyantsev, J.Q. Lu, R. Gaska, M.S. Shur, G. Simin, X. Hu and M. Asif Khan, C.A. Saylor, L.C. Brunel, J. Appl. Phys. **91**, 9346 (2002).
- [14] W. Knap, Y. Deng, S. Romyantsev, M.S. Shur, Appl. Phys. Lett., **81**, 4637 (2002).
- [15] X.G. Peralta, S.J. Allen, M.C. Wanke, N.E. Harff, J.A. Simmons, M.P. Lilly, J.L. Reno, P.J. Burke, and J.P. Eisenstein, Appl. Phys. Lett. **81**, 1627 (2002).
- [16] Taiichi Otsuji, Mitsuhiro Hanabe, and Osamu Ogawara, Appl. Phys. Lett. **85**, 2119 (2004).
- [17] F. Teppe, D. Veksler, V.Yu. Kachorovskii, A.P. Dmitriev, S. Romyantsev, W. Knap, and M.S. Shur, Appl. Phys. Lett., **87**, 052107 (2005).
- [18] F. Teppe, D. Veksler, V.Yu. Kachorovskii, A.P. Dmitriev, X. Xie, X.-C. Zhang, S. Romyantsev, W. Knap, and M.S. Shur, Appl. Phys. Lett. **87**, 022102 (2005).
- [19] D. Veksler, F. Teppe, A. P. Dmitriev, V. Yu. Kachorovskii, W. Knap, and M. S. Shur Phys. Rev. B **73**, 125328 (2006).
- [20] F. Teppe, M. Orlov, A. El Fatimy, A. Tiberj, W. Knap, J. Torres, V. Gavrilenko, A. Shchepetov, Y. Roelens, and S. Bollaert, Appl. Phys. Lett. **89**, 222109 (2006).
- [21] A. El Fatimy, F. Teppe, N. Dyakonova, W. Knap, D. Seliuta and G. Valuis, A. Gotauto, A. Shchepetov, Y. Roelens, S. Bollaert, A. Cappy, S. Romyantsev, Appl. Phys. Lett. **89**, 131926 (2006).
- [22] W. Knap, F. Teppe, Y. Meziani, N. Dyakonova, J. Lusakowski, F. Boeuf, T. Skotnicki, D. Maude, S. Romyantsev, M. S. Shur, Appl. Phys. Lett. **85**, 675 (2004).
- [23] R. Tauk, F. Teppe, S. Boubanga, D. Coquillat, W. Knap, Y. M. Meziani, C. Gallon, F. Boeuf, T. Skotnicki, C. Fenouillet-Beranger, D. K. Maude, S. Romyantsev and M. S. Shur, Appl. Phys. Lett. **89**, 253511 (2006).
- [24] A. El Fatimy, S. Boubanga Tombet, F. Teppe, W. Knap, D.B. Veksler, S. Romyantsev, M.S. Shur, N. Pala, R. Gaska, Q. Fareed, X. Hu, D. Seliuta, G. Valusis, C. Gaquiere, D. Theron, and A. Cappy, Electronics Letters **42**, 1342 (2006).
- [25] V. Yu. Kachorovskii, M. S. Shur, Appl. Phys. Lett. **100**, 232108 (2012).
- [26] T. Otsuji and M. Shur, IEEE Microw. Mag. **15**, 43 (2014).
- [27] M. S. Shur, Proc. SPIE **9467**, 94672A (2015).
- [28] A. El Fatimy, N. Dyakonova, Y. Meziani, T. Otsuji, W. Knap, S. Vandenbrouk, K. Madjour, D. Theron, C. Gaquiere, M. A. Poisson, S. Delage, P. Prystawko, and C. Skierbiszewski, J. App. Phys. **107**, 024504 (2010).
- [29] A. Lisauskas, U. Pfeiffer, E. Öjefors, P.H. Bolivar, D. Glaab, and H.G. Roskos, J. Appl. Phys. **105**, 114511 (2009).
- [30] R. Appleby and H.B. Wallace, IEEE Trans. Antennas Propag. **55**, 2944 (2007).
- [31] T. Otsuji, V. Popov, and V. Ryzhii, J. Phys. D. **47**, 094006 (2014).
- [32] W. Knap, Y. Deng, S. Romyantsev, and M. S. Shur, Appl. Phys. Lett. **81**, 4637 (2002).
- [33] S. Boppel, A. Lisauskas, V. Krozer, and H. Roskos, Electron. Lett. **47**, 661 (2011).
- [34] F. Schuster, D. Coquillat, H. Videlier, M. Sakowicz, F. Teppe, L. Dussopt, B. Giffard, T. Skotnicki, and W. Knap, Opt. Express **19**, 7827 (2011).
- [35] V. Yu. Kachorovskii and M. S. Shur, Solid-State Electronics **52**, 182 (2008).
- [36] B. Gershgorin, V. Yu. Kachorovskii, Y. V. Lvov, and M. S. Shur, Electronics Lett. **44**, 1036 (2008).
- [37] S. Preu, S. Kim, R. Verma, P. G. Burke, N. Q. Vinh, M. S. Sherwin, and A. C. Gossard, IEEE Trans. THz Sci. Technol. **2**, 278 (2012).
- [38] A. Lisauskas, S. Boppel, M. Mundt, V. Krozer, and Hartmut G. Roskos, IEEE Sensors J. **13n**, 124 (2013).
- [39] S. Blin, P. Nouvel, A. Pnarier, and J. Hesler, IEEE Electron Device Lett. **38**, 20 (2017).
- [40] S. Boppel, A. Lisauskas, A. Max, V. Krozer, and H. G. Roskos, Opt. Lett. **37**, 536 (2012).
- [41] S.L. Romyantsev, X. Liu, V.Yu. Kachorovskii, and M. Shur, Appl. Phys. Lett. **111**, 121105 (2017).
- [42] E. L. Ivchenko and S. D. Ganichev, Pisma Zh. Eksp. Teor. Fiz. **93**, 752 (2011) [JETP Lett. **93**, 673 (2011)].
- [43] B. Sothmann, R. Sánchez, A. N. Jordan, and M. Büttiker, Phys. Rev. B **85**, 205301 (2012).
- [44] A. V. Nalitov, L. E. Golub, and E. L. Ivchenko, Phys. Rev. B **86**, 115301 (2012).
- [45] V. V. Popov, Appl. Phys. Lett. **102**, 253504 (2013).
- [46] I. V. Rozhansky, V. Yu. Kachorovskii, and M. S. Shur, Phys. Rev. Lett. **114**, 246601 (2015).
- [47] A. Gutin, V. Yu. Kachorovskii, A. Muraviev, M. Shur, J. Appl. Phys. **112**, 014508 (2012).
- [48] A. Gutin, T. Ytterdal, V. Kachorovskii, A. Muraviev, and M. Shur, IEEE Sensors J. **13**, 55 (2013).
- [49] V. Yu. Kachorovskii, S. L. Romyantsev, W. Knap, M. Shur, Appl. Phys. Lett. **102**, 223505 (2013).
- [50] C. Drexler, N. Dyakonova, P. Olbrich, J. Karch, M. Schafberger, K. Karpierz, Yu. Mityagin, M. B. Lifshits, F. Teppe, O. Klimenko, Y. M. Meziani, W. Knap, and S. D. Ganichev, J. Appl. Phys. **111**, 124504 (2012).
- [51] K. S. Romanov and M. I. Dyakonov Applied Phys. Lett. **102**, 153502 (2013).
- [52] A.V. Chaplik, Zh. Eksp. Teor. Fiz., **62**, 746 (1972)[Sov. Phys. JETP **35**, 395 (1972)].
- [53] Since we consider here resonant case, we neglect smooth dependence of  $U_a$  and  $U_b$  on frequency which might arise due to frequency dependence of the loading impedances.
- [54] These terms can be safely neglected keeping only quadratic order with respect to  $U_{a,b}$ , and considering zero dc current in the channel. For discussion of a more general situation see Refs. [19, 36, 47, 48].